Water Resources Research

RESEARCH ARTICLE
10.1029/2023WR036706

The Fragility of Bedform-Induced Hyporheic Zones: Exploring Impacts of Dynamic Groundwater Table Fluctuations

L. Wu[1,2,3], J. D. Gomez-Velez[4], L. Li[1,2], and K. C. Carroll[5]

[1]Institute of Advanced Technology, Westlake Institute for Advanced Study, Hangzhou, China, [2]Key Laboratory of Coastal Environment and Resources of Zhejiang Province, School of Engineering, Westlake University, Hangzhou, China, [3]Department of Health and Environmental Sciences, Xi'an Jiaotong-Liverpool University, Suzhou, China, [4]Environmental Sciences Division & Climate Change Science Institute, Oak Ridge National Laboratory, Oak Ridge, TN, USA, [5]Department of Plant and Environmental Sciences, New Mexico State University, Las Cruces, NM, USA

Abstract Hyporheic zones are commonly regarded as resilient and enduring interfaces between groundwater and surface water in river corridors. In particular, bedform-induced advective pumping hyporheic exchange (bedform-induced exchange) is often perceived as a relatively persistent mechanism in natural river systems driving water, solutes, and energy exchanges between the channel and its surrounding streambed sediments. Numerous studies have been based on this presumption. To evaluate the persistence of hyporheic zones under varying hydrologic conditions, we use a multi-physics framework to model advective pumping bedform-induced hyporheic exchange in response to a series of seasonal- and event-scale groundwater table fluctuation scenarios, which lead to episodic river-aquifer disconnections and reconnections. Our results suggest that hyporheic exchange is not as ubiquitous as generally assumed. Instead, the bedform-induced hyporheic exchange is restricted to a narrow range of conditions characterized by minor river-groundwater head differences, is intermittent, and can be easily obliterated by minor losing groundwater conditions. These findings shed light on the fragility of bedform-induced hyporheic exchange and have important implications for biogeochemical transformations along river corridors.

Plain Language Summary The hyporheic zone is a small veneer connecting surface water and groundwater systems, which supports vital ecosystem services along river corridors. The current paradigm assumes this exchange zone is ubiquitous and relatively stable over space and time. Yet, the dynamic nature of the surface and subsurface process driving and modulating the exchange can lead to complex spatiotemporal dynamics where bedform-induced hyporheic zones are only present for short periods or are absent. In this study, we investigated how persistent hyporheic zones are under typical groundwater dynamics. We found that bedform-induced hyporheic zones are not as stable as usually assumed, and their presence is restricted to a narrow range of hydrological conditions. The findings reveal the fragility of hyporheic zones and offer new perspectives to conceptualize river connectivity processes.

Key Points:

- We explore bedform-induced hyporheic exchange under various seasonal- and event-scale groundwater table fluctuation scenarios
- Bedform-induced exchange is intermittent and limited to a narrow range of conditions where river-groundwater head differences are small
- Bedform-induced exchange fragility highlights the need for better representations of turbulence and turnover drivers in water quality models

Supporting Information:

Supporting Information may be found in the online version of this article.

Correspondence to:

L. Wu and J. D. Gomez-Velez,
liwen.wu@xjtlu.edu.cn;
gomezvelezjd@ornl.gov

Citation:

Wu, L., Gomez-Velez, J. D., Li, L., & Carroll, K. C. (2024). The fragility of bedform-induced hyporheic zones: Exploring impacts of dynamic groundwater table fluctuations. *Water Resources Research*, *60*, e2023WR036706. https://doi.org/10.1029/2023WR036706

Received 13 NOV 2023
Accepted 14 JUN 2024

Author Contributions:

Conceptualization: L. Wu, J. D. Gomez-Velez, K. C. Carroll
Data curation: L. Wu, J. D. Gomez-Velez
Formal analysis: L. Wu, J. D. Gomez-Velez
Funding acquisition: J. D. Gomez-Velez, L. Li, K. C. Carroll
Investigation: L. Wu, J. D. Gomez-Velez, K. C. Carroll
Methodology: L. Wu, J. D. Gomez-Velez
Software: L. Wu, J. D. Gomez-Velez
Supervision: J. D. Gomez-Velez, L. Li, K. C. Carroll
Validation: L. Wu, J. D. Gomez-Velez

1. Introduction

The hyporheic exchange zone is a dynamic interface connecting rivers and aquifers, playing a critical role in river corridor ecosystem services (Boulton, 2003; Gómez-Gener et al., 2021; Harvey & Gooseff, 2015; Harvey et al., 2018; Krause et al., 2017, 2022; Stanley et al., 1997). This exchange has traditionally been assumed as a resilient process contributing to the emergence of hotspots and hot moments for biogeochemical processes in river corridors (McClain et al., 2003; Newcomer et al., 2018; Stegen et al., 2016, 2018), leading to significant efforts to understanding its role in nutrient cycling (i.e., carbon, nitrogen, and oxygen), greenhouse gas emissions (Son, Fang, Gomez-Velez, Byun, & Chen, 2022; Son, Fang, Gomez-Velez, & Chen, 2022), contaminant fate and transport, and microbiome dynamics over different spatial (Claret & Boulton, 2009; Gomez-Velez et al., 2015) and temporal (Briggs et al., 2014; Gomez-Velez et al., 2017; Gu et al., 2012) scales.

Central to understanding the role of the hyporheic zone in biogeochemical transformations is the characterization of the physical processes driving and modulating the exchange process and constraining its characteristic time scales. This study concentrates on the hyporheic exchange induced by bedform-driven pumping. While meander-driven hyporheic exchange also holds significance, it warrants a separate investigation and will not be addressed

Visualization: L. Wu, J. D. Gomez-Velez, K. C. Carroll
Writing – original draft: L. Wu
Writing – review & editing: J. D. Gomez-Velez, L. Li, K. C. Carroll

within the scope of this paper. The main mechanisms driving bedform-induced hyporheic exchange include (a) spatial variation in near-bed pressure head (bedform-induced advective pumping), (b) near-bed turbulence, and (c) bedload transport (turnover) (Boano et al., 2014; Buffington & Tonina, 2009; Tonina & Buffington, 2009). Even though these processes co-occur, and their relative importance depends on channel hydraulic conditions, streambed properties, and regional groundwater flow (hereafter understood as the boundary fluxes contributed by the overall groundwater fluxes from the lower streambed), bedform-induced advective pumping has received significantly more attention (Boano et al., 2014; Grant et al., 2018; Schulz et al., 2023; Wu et al., 2020) and is at the core of most upscaling frameworks for hyporheic exchange (e.g., Azizian et al., 2015, 2017; Elliott & Brooks, 1997; Gomez-Velez & Harvey, 2014a; Herzog et al., 2019; Marzadri et al., 2011, 2014; Perez et al., 2021; Stonedahl et al., 2010, 2012, 2013; Wörman et al., 2006, 2007). This emphasis can be partially explained by its intuitive conceptualization.

The impact of all these driving mechanisms is modulated by the regional groundwater (Malzone et al., 2016; Wu et al., 2021) and local geomorphological settings (Caruso et al., 2016; Gomez-Velez & Harvey, 2014b; Tonina & Buffington, 2011). In particular, regional groundwater flow can significantly diminish the hyporheic exchange and its biogeochemical potential (Azizian et al., 2015, 2017). For example, a recent study by Bonanno et al. (2023) showed that the dynamics of regional groundwater fluxes can lead to periods where the exchange process is undetectable in tracer tests. This contradicts the typical assumption that hyporheic zones are persistent as long as water is present in the river channel. Mechanistically, this regional groundwater contribution (either gaining or losing) is likely affecting all exchange drivers, with the bedform-induced advective pumping succumbing first due to its high sensitivity to exogenous fluxes (Azizian et al., 2017; Boano et al., 2008; Cardenas & Wilson, 2007b; Caruso et al., 2016). Wondzell (2011) found that the role of the hyporheic zone in stream ecosystems changes with both location within the stream network as well as with seasonal or storm-driven changes in discharge, suggesting that hyporheic exchange is highly variable in place and time, and geomorphological settings regulate the hyporheic exchange processes.

Climate change and increasing population have led to increasing water demand and groundwater withdrawal, which may eventually contribute to decreased river flow and lowered groundwater table (Heidari et al., 2021; Jasechko et al., 2021). Ephemeral or intermittent streams, especially in semi-arid regions, can be caused or enhanced by climate disturbances such as drought (Hammond et al., 2021; Zipper et al., 2021), and these systems may undergo extreme hydrologic transitions from connection to disconnection (Fuchs et al., 2019; Pearson et al., 2022).

Given the strong modulating effects of regional groundwater fluxes, it is imperative to assess the limiting range of gaining, losing, and disconnected river-aquifer conditions under which hyporheic zones persist or even exist. The spatial distribution of infiltration and seepage through a surface water source depends on the state of connection (Brunner, Cook, & Simmons, 2009; Brunner, Simmons, & Cook, 2009; Pearson et al., 2022; Quichimbo et al., 2020; Shanafield et al., 2012), which can be paramount to understanding biogeochemical cycling of nutrients and pollutants within the hyporheic zone (Findlay, 1995; Krause et al., 2011; Shabaga & Hill, 2010). Some rivers can have transitions between a gaining-river and losing-river systems (Wroblicky et al., 1998) and a single river can comprise some gaining reaches and other locations under losing conditions. Most, if not all, of the previous hyporheic studies are focused on connected and completely saturated conditions.

Although the general idea that strong vertical head gradients tend to reduce or eliminate small-scale exchange due to bed-current interactions has been known and quantified for over a decade (Boano et al., 2008; Cardenas & Wilson, 2006; Sawyer & Cardenas, 2012), these evaluations have not been extended to explore the situations with transient dynamic groundwater table fluctuations, particularly in arid and semi-arid regions where river-aquifer disconnection and re-connection may occur. In agreement with the studies mentioned above, we build on this work by exploring what happens for hyporheic exchange in situations where dynamic groundwater table fluctuations can lead to temporary disconnections between surface water and groundwater, and the formation of partially saturated zones. In this study, we examine the persistence of hyporheic zones driven by bedform-induced advective pumping under varying hydrological scenarios with both saturated and unsaturated streambed conditions. To this end, we propose a multi-physics framework to study how hyporheic zones respond to different degrees of river-groundwater connections and disconnections and address the following questions: (a) are bedform-induced hyporheic zones persistent under typical seasonal- and event-scale groundwater table

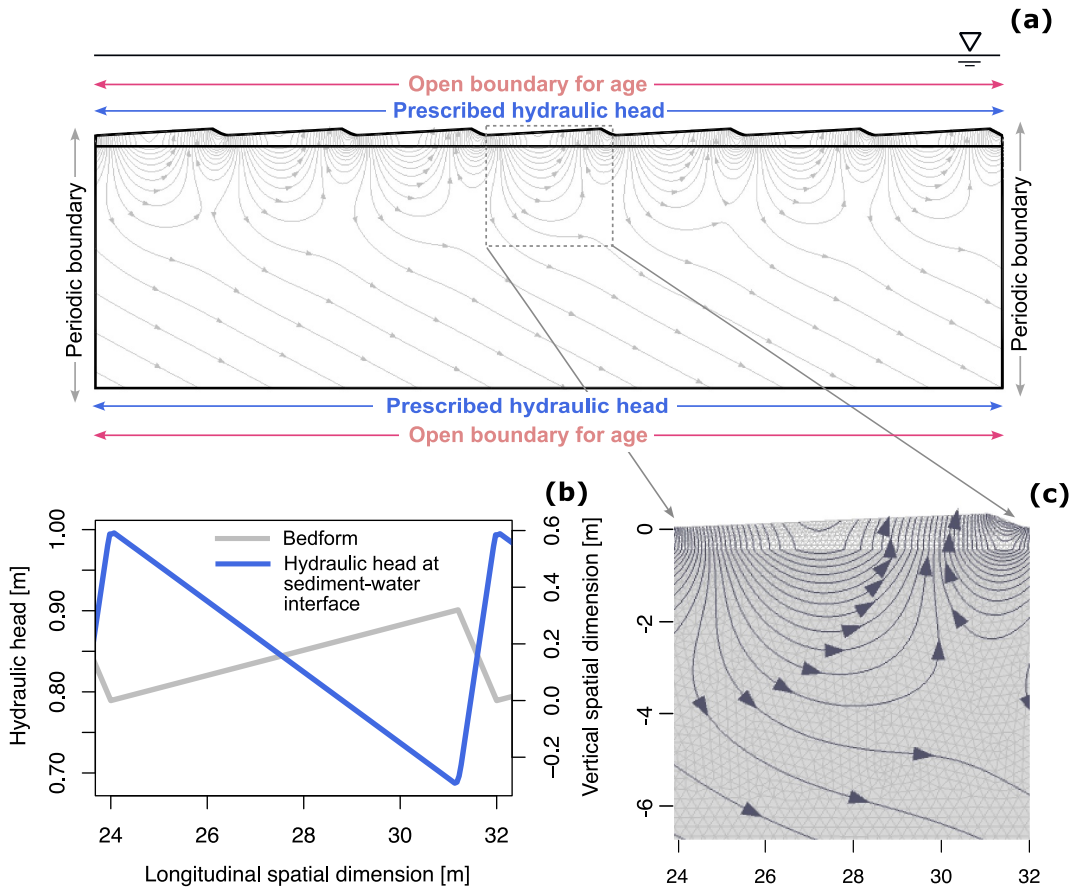

Figure 1. (a) Conceptual diagram of the modeling domain. For the flow model, we prescribe the hydraulic head at the upper and lower boundaries (blue arrows); for the mean age model, we use an open boundary condition (red arrows). An open boundary imposes a prescribed mean age for fluxes entering the domain and an advective boundary condition for fluxes leaving the domain. The lateral boundaries are the periodic boundaries. (b) Bedform (gray line) and simulated hydraulic head at the water-streambed interface (blue line). (c) Inset of the hyporheic circulation cells at the length scale of one bedform.

fluctuations? (b) what are the characteristic time scales of the hyporheic exchange fluxes? (c) what are the windows or ranges of hydraulic heads that activate hyporheic exchange?

2. Methods

2.1. Conceptual Description

We use a multi-physics framework to model the evolution of water flow and mean water age within a modeling domain representative of the porous media underneath a sequence of periodic dune bedforms (Figure 1a). The scale of investigation is representative of both laboratory flumes and small stream reach lengths that would include dune bedforms. Dune geometry can vary significantly in natural channels (Bridge, 2003). In our case, we use the empirical relationships from Yalin (1972) and Yalin and Da Silva (2001) to propose values for the bedform geometry. With these relationships, we obtain an aspect ratio of 0.04 consistent with empirical observations (see, e.g., Figure 6 in Venditti, 2013) and a length and height are within the range of empirical scaling relationships (see, e.g., Figure 5 in Venditti, 2013). The aspect ratio is the main factor affecting the pressure fluctuations at the sediment-water interface. Like Brunner, Cook, and Simmons (2009), the porous media is conceptualized as a homogeneous and isotropic two-layered system representative of the streambed and the underlying alluvial aquifer sediments. The streambed sediments are bounded at the top by the water-streambed interface (WSI) and constitute a lower-permeability layer (i.e., clogging layer or streambed sediments) that overlies the higher-permeability alluvial aquifer.

The conceptual setting of a lower permeability riverbed overlying more permeable alluvial sediments is only one of many possible natural river sediment settings. There are cases where a higher permeability sediment layer is on top of the low-permeability aquifer layer. In these cases, the unsaturated layer would not be able to develop between these two layers. The drying process will start from the top of the sediment once the water in the river channel is completely drained (Brunner, Cook, & Simmons, 2009). In this study, we focus on the scenario in which a lower permeability streambed layer is overlying a higher permeability aquifer layer, where disconnection between surface water and groundwater can occur, since it is more of interest in arid and semi-arid regions. In our configuration, the streambed is the clogging layer that enables the perching of the surface water above the underlying groundwater table. This may be common for depositional systems with grain-size sorting and fines deposited at the end of intermittent river flows.

In this case, channel flow over the bedforms results in periodic hydraulic head gradients at the WSI (blue line in Figure 1b) that drive exchange between the channel and the porous media and can result in the emergence of circulation flow cells with streamlines that start and end at the WSI (Figure 1c). These flow cells are the *bedform-induced advective pumping hyporheic zones* (Boano et al., 2014; Elliott & Brooks, 1997; Gooseff, 2010; Tonina & Buffington, 2009). For convenience, it's written as *bedform-induced hyporheic zones* below. Both the exchange process and the resulting bedform-induced hyporheic zones are continuously modulated by regional groundwater fluxes. These fluxes are driven by water table fluctuations that can lead to episodic disconnections between the channel and the alluvial aquifer. As model results herein show, the nature of the bedform-induced hyporheic zones strongly depends on the dynamic interplay between the surface water and regional groundwater processes. The flow simulations carefully track the evolution of the hyporheic flow lines to describe the bedform-induced hyporheic zone dynamics and calculate hyporheic fluxes and flux-weighted mean ages. In this study, we use regional groundwater to refer to the boundary fluxes contributed by the overall groundwater fluxes from the lower boundary. For simplicity, different sources of groundwater are not distinguished but collectively called regional groundwater.

In the following subsections, we present a detailed description of the flow and mean age models, including complete mathematical statements and their physical rationale.

2.2. Water Flow Model

We use a sequential approach to couple flow in the channel's water column with the flow in the porous media domains (see, e.g., Cardenas & Wilson, 2007b; Gomez-Velez et al., 2014). In this case, we model turbulent transport in the water column and prescribe the resulting pressure distribution along the WSI as a Dirichlet boundary condition for the porous media model.

2.2.1. Turbulent Flow in the Surface Water Column Domain

To capture the pressure distribution along the WSI, we model the surface water flow with a Reynolds-averaged Navier-Stokes approach. In this case, flow is assumed steady state, and we prescribe the mean flow velocity and water depth. The turbulence effects are modeled using the Menter Shear-Stress Transport (SST) model, which can resolve near-wall turbulence without wall function approximations (BV & OY, 1998; Menter, 1994) and provides a more accurate description of the pressure distributions along the WSI. For brevity, the details of the computational fluid dynamics model and its equations are described in Supplemental Information S1.

2.2.2. Unsaturated Flow in the Porous Media Domain

As mentioned before, the interplay between the water column and regional groundwater systems can lead to the disconnection of the surface water-groundwater continuum. This disconnection results in the emergence of unsaturated water flow and the formation of a perched water table (Bear, 1972; Brunner, Cook, & Simmons, 2009; Stephens, 1994; Xie et al., 2014). To capture this complex behavior, we use the Richards equation to model water flow through variably saturated porous media (Bear, 1972; Richards, 1931):

$$(C_m + S_e S)\frac{\partial H_p}{\partial t} + \nabla \cdot [-K k_r (\nabla H_p + \nabla z)] = Q_m \quad (1)$$

where t is time [T], $\mathbf{x}$ is the spatial coordinate vector [L], C_m is the specific moisture capacity [L^{-1}], $S_e(\mathbf{x}, t) = (\theta - \theta_r)/(\theta_s - \theta_r)$ is the effective saturation [−], $\theta(\mathbf{x}, t)$ is the volumetric water content [−], θ_r is the residual water content [−], θ_s is the saturated water content [−], S is the storage coefficient [L^{-1}], H_p is the pressure head [L], t is time [T], K is the saturated hydraulic conductivity [LT^{-1}], $k_r(\mathbf{x}, t)$ is the relative permeability [−], z is the elevation [L], and Q_m is the fluid source or sink. The Darcy flux is defined as $\mathbf{q} = -K\, k_r\, (\nabla H_p + \nabla z)$ [LT^{-1}].

The Richards equation is notoriously nonlinear, where the nonlinearities lie in the porous media hydraulic properties θ, S_e, C_m, and k_r that vary with fluid saturation. In this work, we use the empirical expression proposed by Van Genuchten (1980):

$$\theta = \begin{cases} \theta_r + S_e(\theta_s - \theta_r) & H_p < 0 \\ \theta_s & H_p \geq 0 \end{cases} \tag{2a}$$

$$S_e = \begin{cases} (1 + |\alpha H_p|^n)^{-m} & H_p < 0 \\ 1 & H_p \geq 0 \end{cases} \tag{2b}$$

$$k_r = \begin{cases} S_e^l \left[1 - \left(1 - S_e^{1/m}\right)^m\right]^2 & H_p < 0 \\ 1 & H_p \geq 0 \end{cases} \tag{2c}$$

$$C_m = \begin{cases} \dfrac{\alpha\, m}{1 - m} (\theta_s - \theta_r)\, S_e^{1/m} \left(1 - S_e^{1/m}\right)^m & H_p < 0 \\ 0 & H_p \geq 0 \end{cases} \tag{2d}$$

where α [L^{-1}], n [−], m [−], and l [−] are constitutive parameters. Here, we use the parameter values from Brunner, Cook, and Simmons (2009) (see Table 1).

Our modeling domain includes a sequence of seven dunes with length L, and we focus our analyses on the middle dune to avoid boundary effects. We prescribe hydraulic heads at the top and bottom boundaries (Figure 1). At the WSI, the hydraulic head is given by the computational fluid dynamic flow model of the water column. At the bottom boundary, a time-varying hydraulic head is imposed. The functional forms of this boundary signal resemble different climatic drivers and are described in Section 2.4. Finally, the lateral boundaries are periodic with a head drop of $7L \cdot S$, mimicking an infinite periodic domain. Initial conditions are obtained with a spin-up process, where the flow field is simulated until it reaches a dynamic equilibrium.

We use the solution to the flow model to delineate hyporheic streamlines (i.e., start and end at the WSI). Once these are identified, we defined the boundary at the WSI where the hyporheic exchange was taking place: $\partial\Omega_{HZ}(t)$. This subset of the WSI is time-varying and depends on the boundary conditions. Furthermore, it can be subdivided into sections where water enters the hyporheic zone from the channel ($\partial\Omega_{HZ,in}(t)$) and sections where water leaves the hyporheic zone and is discharged into the channel ($\partial\Omega_{HZ,out}(t)$). Then, the net hyporheic exchange per unit of channel width is calculated as:

$$Q_{HZ}(t) = \int_{\partial\Omega_{HZ,in}(t)} -\mathbf{n} \cdot \mathbf{q}\, d\mathbf{x} \tag{3}$$

where $\mathbf{n}$ is an outward vector normal to the WSI.

2.3. Model for Mean Water Age

To characterize the typical time scales for the exchange process, we model the spatiotemporal evolution of the mean water age, which is described by the following advection-dispersion equation (Ginn, 1999; Gomez-Velez & Wilson, 2013):

$$\frac{\partial(\theta a)}{\partial t} = \nabla \cdot (\mathbf{D} \nabla a) - \nabla \cdot (\mathbf{q} a) + \theta \tag{4}$$

Table 1
Parameter Setting in the Numerical Simulations

Parameter	Value	Description
Water Column		
U	0.1 m/s	Mean channel velocity
d	1 m	Channel depth
Bedform Geometry		
L	8 m	Bedform length
L_c	0.9 L	Bedform stoss length
H	0.32 m	Bedform height
d_s	0.5 m	Streambed depth
S	0.001	Channel slope
Porous Media Properties		
θ_a	0.43	Aquifer porosity
θ_s	0.25	Streambed porosity
$\theta_{a,r}$	0.045	Aquifer residual water content
$\theta_{s,r}$	0.078	Streambed residual water content
K_a	10^{-4} m/s	Aquifer sat. hyd. conductivity
K_s	10^{-6} m/s	Streambed sat. hyd. conductivity
α_L	$L/20$	Longitudinal dispersivity
α_T	$\alpha_L/10$	Transverse dispersivity
α_a	14.5 m^{-1}	Parameter α for aquifer
α_s	3.6 m^{-1}	Parameter α for streambed
n_a	2.68 m^{-1}	Parameter n for aquifer
n_s	1.56 m^{-1}	Parameter n for streambed
Fluid Properties		
ρ	1,000 kg/m^3	Density
μ	1.002×10^{-3} Pa·s	Dynamic viscosity
D_m	10^{-9} m^2/s	Molecular diffusion coefficient

where $a(\mathbf{x}, t)$ is the mean age of water [T] and $\mathbf{D} = \{D_{i,j}\}$ is the dispersion-diffusion tensor [L^2T^{-1}]. The dispersion-diffusion tensor is defined as

$$D_{i,j} = \alpha_T |\mathbf{q}| \delta_{i,j} + (\alpha_L - \alpha_T) \frac{q_i q_j}{|\mathbf{q}|} + \frac{\theta}{\eta} D_m \tag{5}$$

with α_T and α_L the transverse and longitudinal dispersivities [L], respectively, $\delta_{i,j}$ the Kronecker delta function [−], D_m the molecular diffusion [L^2T^{-1}], and $\eta = \epsilon_p^{-1/3}$ the tortuosity factor approximated with the Millington and Quirk model (Millington & Quirk, 1961).

By definition, water entering the domain through the WSI is "new" water and has a mean age of zero ($a = 0$). On the other hand, for water leaving the porous media and discharging into the water column, we assume an advective boundary such that $-\mathbf{D}\nabla a = 0$. Lateral boundaries are periodic to mimic an infinite periodic domain (i.e., $a(x = 0, y, t) = a(x = 7\text{L}, y, t)$). We assume, without loss of generality, that the bottom boundary has a prescribed mean age of 1 year (see, e.g., Gomez-Velez et al., 2014) for water entering the modeling domain and an advective boundary for water leaving the domain. The flow and mean age models are solved in sequence. First, we solve the flow model until a dynamic equilibrium is reached. Then, this flow field is used to spin up the mean age model, similar to the flow field spin-up process. Note that dispersivity is a critical parameter for characterizing solute transport in the sediment (Hester et al., 2013, 2017). In this study, the dispersivity is used for simulating mean age distribution. Along with other assumptions (i.e., groundwater age of 1 year), the simulated flux-weighted mean age provides an approximation for understanding the mean age variations responding to the groundwater table fluctuations.

As a measure of the typical time scales of hyporheic exchange, we calculate the flux-weighted mean age for hyporheic water discharging into the surface water column:

$$a_{HZ}(t) = \frac{\int_{\partial\Omega_{HZ,out}(t)} -(\mathbf{n}\cdot\mathbf{q})\, a \, d\mathbf{x}}{\int_{\partial\Omega_{HZ,out}(t)} -(\mathbf{n}\cdot\mathbf{q})\, d\mathbf{x}}. \tag{6}$$

Here, it is important to note that the mean age of water in groundwater systems with nested flow systems is typically characterized by a heavy-tailed probability distribution for age (Cardenas, 2007, 2008). In addition, flow dynamics further increases the role of the distribution tails and leads to the emergence of additional modes in the distribution (Gomez-Velez & Wilson, 2013; Gomez-Velez et al., 2017). The impact of heavy tails and multi-modality in the age distribution tends to bias the mean age, which is the first moment of such distribution, toward older ages. Therefore, in this study, we use the mean age as a proxy for changes in time scales but avoid using this metric as the dominant age of hyporheic waters.

2.4. Modeling Scenarios

To capture typical weather-controlled groundwater table fluctuation patterns for arid and semi-arid environments, two scenarios are selected based on Newcomer et al. (2018). First, a *groundwater average* scenario that represents a seasonal fluctuation pattern under which river and aquifer seasonally undergo disconnection and reconnection (Figure 2a). Second, an *atmospheric river* scenario that represents a long-term dry losing period punctuated by short periods of river-aquifer reconnection due to extreme storm events (Figure 2b).

Groundwater average and atmospheric river scenarios characterize the groundwater table fluctuation patterns and include transitions from gaining to losing with connected surface water-groundwater and also transition to disconnection. To further describe the average hydraulic head difference between the river and aquifer at the

10.1029/2023WR036706

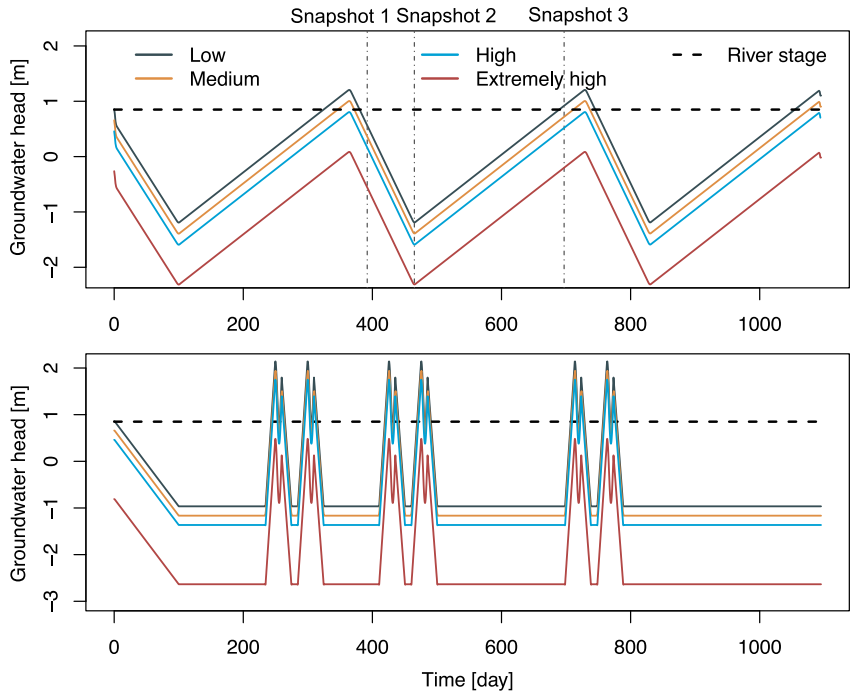

Figure 2. Simulation scenarios and cases. (a) Groundwater average scenario with four cases: low, medium, high, and extremely high cases. The horizontal dash line is the spatially averaged river head. The vertical dash-dot line indicates three snapshots in time for the comparisons in Figure 3. (b) Atmospheric river scenario with four cases: low, medium, high, and extremely high cases. These four cases represent gradually declining groundwater table and increasing hydraulic head differences between the river and underlying groundwater.

bottom model boundary, four cases are created for each scenario with a gradually lowered average groundwater table representing a gradually increased river-aquifer hydraulic head difference. These four cases are *low*, *medium*, *high*, and *extremely high* in terms of groundwater elevation decline and hydraulic head difference between the river and underlying groundwater. In the low case, the groundwater table at the bottom boundary fluctuates from values relatively close to the river head, creating no obvious gaining or losing regional fluxes at the beginning of the groundwater table fluctuations. With decreasing average groundwater table elevations in the medium and high cases, hydraulic head differences between river and aquifer are increased, resulting in longer losing and disconnected river-aquifer conditions. In the extremely high case, river water is continually lost to the underlying aquifer, and hyporheic exchange barely occurs even when the hydraulic head at the bottom boundary is highest, which is the closest to the river head.

The river stage and flow velocity are kept constant for all simulations. This approach of constant river head with lowering of the water table or groundwater hydraulic head to cause head gradient requirements for transitions from connected to disconnected conditions is commonly used in modeling work (Brunner, Cook, & Simmons, 2009; Brunner, Simmons, & Cook, 2009; Brunner et al., 2011; Irvine et al., 2012; Rivière et al., 2014; Xian et al., 2017, 2019). In this work, the groundwater table fluctuations create a suitable range to hydraulic head differences between surface water and groundwater. These suitable ranges (presented in Equation 6) enable characterization of the persistence of hyporheic zones under temporary connection and disconnection between surface water and groundwater systems. In fact, a relatively constant river stage can be commonly found in rivers and streams that are regulated by reservoir operations in semiarid environments (Pearson et al., 2022). Additionally, this simplification allows us to focus on groundwater dynamics.

Additional simulations with both varying river stages (observed in Rio Grande at Alameda Bridge at Alameda, NM-08329918) and groundwater tables (observed in USGS 351201106400501 11N.03E.07.141 HUNTERS RIDGE NO. 1) are provided to evaluate the validity of this simplification. More information is provided in Supporting Information S1.

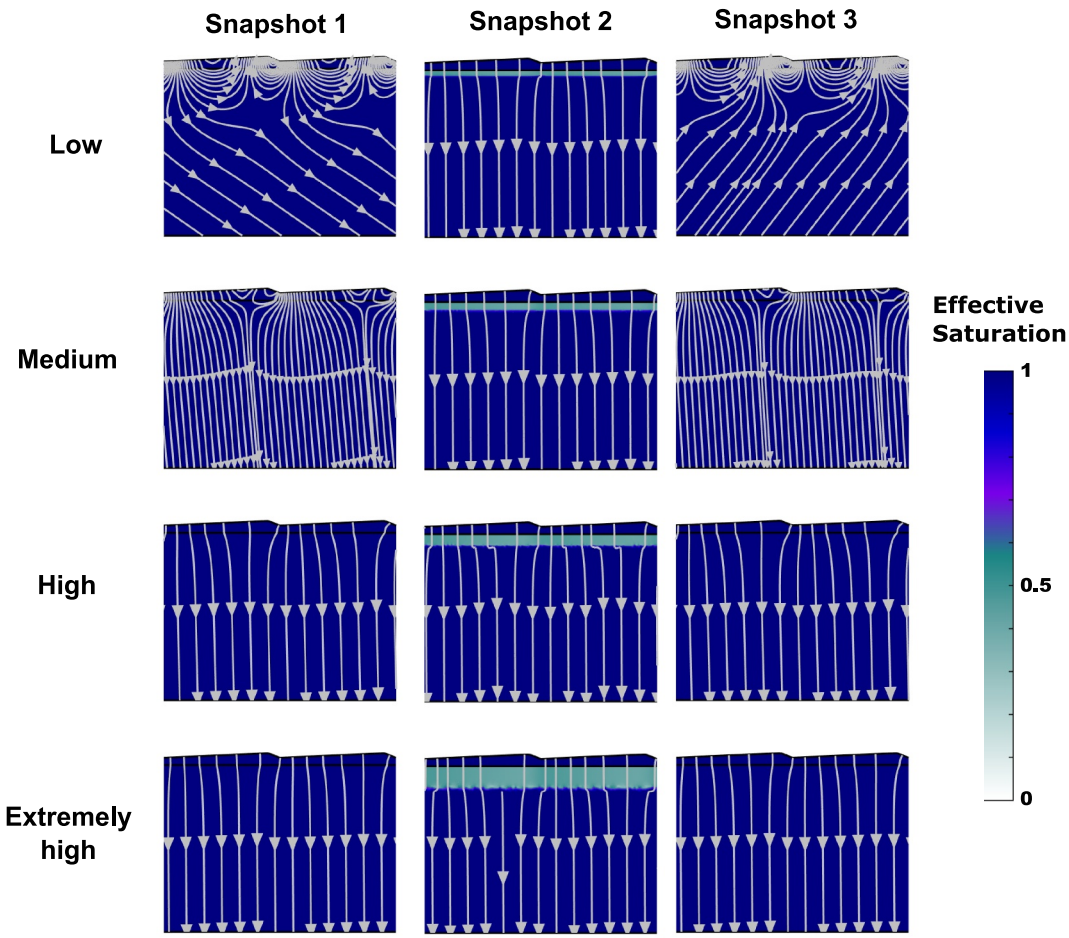

Figure 3. Snapshots of the subsurface flow field and effective saturation for days 392, 465, and 697 (columns; vertical dashed lines in Figure 2a) under low, medium, high, and extremely high scenarios (rows; solid lines in Figure 2a). Disconnection between the river and groundwater systems increases from top to bottom.

3. Results and Discussion

3.1. Bedform-Induced Hyporheic Exchange May Not Be as Ubiquitous as Generally Assumed

The dynamic nature of the groundwater flow is commonly ignored in hyporheic zone studies, where a constant regional groundwater flux and fully saturated conditions are generally assumed (e.g., Azizian et al., 2017; Boano et al., 2008, 2009, 2018; Cardenas, 2007; Cardenas & Wilson, 2007a; Caruso et al., 2016; Gomez-Velez & Harvey, 2014a; Gomez-Velez et al., 2014, 2015). However, the temporal dynamics of groundwater fluxes can have significant implications for the spatiotemporal evolution of the exchange process. In the following, we present a systematic analysis to understand the conditions leading to the emergence of bedform-induced hyporheic flow cells under different degrees of river-aquifer disconnection. In particular, we explore scenarios that mimic seasonal-scale and event-scale groundwater table fluctuations (Figure 2), which induce dynamic behavior in the ambient groundwater flow and the hyporheic exchange process.

First, we focus on the dynamics induced by seasonal groundwater table fluctuations. Figure 3 presents snapshots of the streamlines (encapsulating the flow field) and the effective saturation for three snapshots during one annual cycle (columns) and for different groundwater average cases (rows). Snapshot 1 (day 392) corresponds to a case where the water table starts deepening but is still relatively close to the river head, which results in a slightly losing condition. Snapshot 2 (day 465) is taken when the water table is at its deepest, resulting in the strongest head gradients driving losing conditions. Finally, snapshot 3 (day 697) represents a condition when the water table

recovers and is becoming shallower resulting in modest river-aquifer hydraulic head differences that drive slightly gaining or losing conditions.

For the low case (first row in Figure 3), snapshot 1 shows the formation of hyporheic circulation cells under losing regional groundwater flow. These cells start and end at the streambed-water interface and extend downwards into the streambed layer (with lower hydraulic conductivity) and the aquifer layer (with higher hydraulic conductivity). In snapshot 2, we see the formation of an inverted water table (Stephens, 1994; Xie et al., 2014), where an unsaturated layer (effective saturation lower than one) develops beneath the streambed layer. In this case, surface water recharges the aquifer without circulating back to the river channel. In other words, the bedform-induced hyporheic zone disappears. Finally, in snapshot 3, where the groundwater table recovers to a position slightly higher than the river head, we see the reemergence of hyporheic circulation cells under the modulating effect of a mildly gaining condition.

As the average head difference between the groundwater and river increases (rows 2–4 in Figure 3), the losing groundwater conditions become prevalent throughout the year. Similar to the low case, we see the formation of an inverted water table with its thickness increasing with the magnitude of the average head gradient. The medium case (second row in Figure 3) shows the emergence of modest hyporheic flow cells during snapshots 1 and 3; however, their size is significantly smaller than the ones seen under the low case. As we will show in the following subsections, this is reflected in the total hyporheic exchange flux and its flux-weighted mean age. The reduction in the size of the hyporheic zone is explained by the increase in the groundwater flux as the average head gradient increases, which effectively compresses the cells. This hydrodynamic behavior has been shown under fully saturated conditions (e.g., Azizian et al., 2017; Boano et al., 2008, 2009; Cardenas & Wilson, 2007a; Gomez-Velez et al., 2014). As the average river-groundwater head differences increase, the groundwater flux exceeds the threshold where circulation cells can develop (analogous to Boano et al., 2008; Azizian et al., 2017, for saturated conditions), leading to conditions where the bedform-induced hyporheic zone is permanently absent.

Among the wide range of groundwater scenarios with varying river-groundwater head differences (Figure 2), in only a few cases would hyporheic zones actually form (Figure 3). Only when the groundwater head and the river head are similar in magnitude can hyporheic circulation cells form. Strong gaining or losing conditions can easily obliterate hyporheic zones. This is more evident in the high and extremely high cases, where even during fully saturated conditions (snapshots 1 and 3) no hyporheic zones are present for prolonged periods of time. In other words, hyporheic zones are not always persistent under losing and gaining conditions even when there is water present in the river channel under fully saturated subsurface conditions. In fact, for our simulations, hyporheic zone circulation cells are inhibited under strongly losing conditions and never occur under disconnected surface water-groundwater conditions (extremely high case). These results illustrate the fragility of the hyporheic exchange, which is shown here to only occur in a few cases where the groundwater elevation is closer to the stream without a significant hydraulic head difference. Only when the groundwater head and the river head are relatively close can hyporheic exchange circulation cells form.

3.2. What Are the Temporal Patterns of Bedform-Induced Hyporheic Exchange Fluxes?

To evaluate when and how much hyporheic exchange occurs under different degrees of groundwater-surface water connection during an annual groundwater fluctuation cycle, we estimate the net hyporheic exchange flux and the flux-weighted mean age for the four cases in groundwater average and atmospheric river scenarios.

3.2.1. Groundwater Average Scenario

For the groundwater average scenario, results from day 600 to 900 are presented in Figure 4, and the full-time simulation results are shown in the insets, which mainly illustrate the periodicity of the behavior that supports the focus on individual bedform features.

In the low case, hyporheic exchange fluxes occur when the river and groundwater heads are in close proximity (i.e., minor head differences). During an annual groundwater table fluctuation cycle, the groundwater head (solid gray line) approaches the surface water head (dashed gray line) twice, resulting in two peaks of hyporheic exchange fluxes. The first peak is slightly higher than the second due to the asymmetry of the groundwater table's rising and falling rate. The slope of the groundwater table rising limb is gentler than the slope of the falling limb, therefore more surface water is pushed into the hyporheic zone and returns to the river channel during the

10.1029/2023WR036706

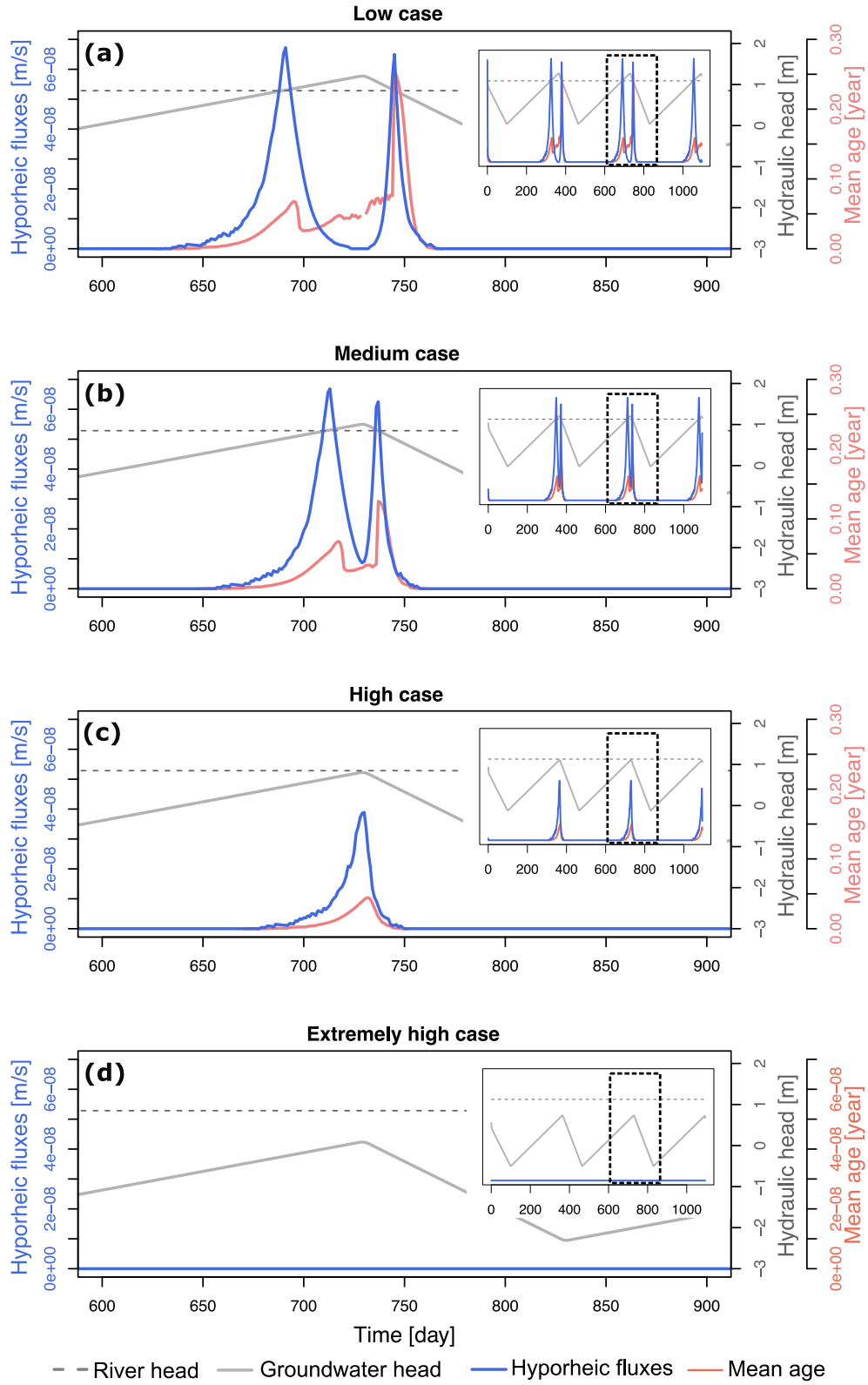

Figure 4. Net hyporheic exchange flux and flux-weighted mean age at different levels of surface water groundwater disconnection for the groundwater average scenario. The river head (dashed gray line) and the groundwater head (solid gray line) are included for reference.

groundwater table rising period. Hyporheic fluxes rapidly become negligible when the groundwater head declines and deviates in magnitude from the river head.

With increasing disconnections between the river and the aquifer in the medium case, there are still two peaks of increased hyporheic fluxes that coincide with the time when the river and groundwater head values are in close proximity, and the magnitude of the hyporheic peaks are similar to that in the low case. These two peaks have increased temporal frequency (or reduced length of time between the peaks) because the two intersections between the groundwater head (gray solid line) and the river head (gray dashed line) in the medium case are closer than that of the low case. As the results indicate, hyporheic exchange fluxes only occur when the groundwater head and the river head are relatively close to each other; the increased temporal frequency between the two intersections of the groundwater head and the river head contributes to the reduced length of time between the two peaks in the hyporheic exchange fluxes.

For the high case, the groundwater head only intersects with the river head once. Therefore, only one peak of the hyporheic exchange flux is shown. For the extremely high case, because the river-groundwater head differences are continually too large to allow for the reversal of the infiltrated surface water flow path, resulting in a continually losing condition, and thus no bedform-induced hyporheic exchange occurs.

The flux-weighted mean age shows similar patterns as the hyporheic exchange fluxes. The mean age peaks are coincident in time with the hyporheic flux peaks. For the low and medium cases, where two age and flux peaks develop, the second mean age peak is higher because during this period the system is flushing both water that entered the hyporheic zone during the first flux peak, which has aged within the sediments, and water that entered during the second, milder flux peak, which is characterized by lower flow rates and longer residence times. Together, these factors result in the flushing of older hyporheic water.

Our results suggest that bedform-induced hyporheic exchange fluxes only occur within a small window of time when the groundwater head is relatively close in magnitude to the river head. This window's length depends on the groundwater table and river stage fluctuation patterns. In this study the river stage is kept constant; the results indicate that the groundwater table fluctuation alone drives the dynamics in the hyporheic exchange processes. Even a mild difference between the river head and the groundwater head can obliterate the hyporheic exchange.

3.2.2. Atmospheric River Scenario

The atmospheric river results, in general, are similar to the average groundwater results shown in Figure 4, but the frequency of groundwater elevation changes is higher and more rapid (Figure 5). Results from day 450 to day 580 are presented in Figure 5, and the full-time simulation results are shown in the insets which again illustrate the periodicity of the behavior. Hyporheic exchange fluxes only occur when the groundwater head approaches the river head. For the low (Figure 5a), medium (Figure 5b), and high cases (Figure 5c), groundwater head approaches river head four times during the observation period, resulting in four peaks of hyporheic exchange fluxes. For the extremely high case (Figure 5d), only at the highest groundwater table position (around day 477) can bedform-induced hyporheic exchange occur, but only in a minor amount.

The magnitude of flux-weighted mean age depends on the antecedent flow conditions. That is, if the previous flow condition is gaining, then the hyporheic flux-weighted mean age would be relatively high due to the mixing with old regional groundwater. On the other hand, if the previous flow condition is losing, the mean age would be relatively low because of the mixing of fresh surface water. Take the high case as an example (Figure 5c), from day 460 to 500, with the groundwater table fluctuations (gray solid line), the system goes from losing to gaining, then to losing, and again to gaining to losing. The second hyporheic flux peak is after a gaining condition, and the third hyporheic flux peak is after a losing condition, therefore the magnitude of flux-weighted mean age at the second peak is higher than the third peak.

In the atmospheric scenario, the groundwater losing-disconnected period is punctuated by short periods of transitional losing-to-gaining conditions due to the impact of storm events. These short transitional periods create temporary connections and therefore hyporheic exchange fluxes. Compared with the groundwater average scenario, the higher groundwater table fluctuation frequency results in the formation of additional hyporheic flux and flux-weighted mean age peaks. Again, the flux peak timing always coincides with the time when the river and groundwater head values are in close proximity, the magnitude of the hyporheic peaks are similar, and hyporheic fluxes rapidly become negligible aside from these peaks. The main difference for the atmospheric river scenarios,

10.1029/2023WR036706

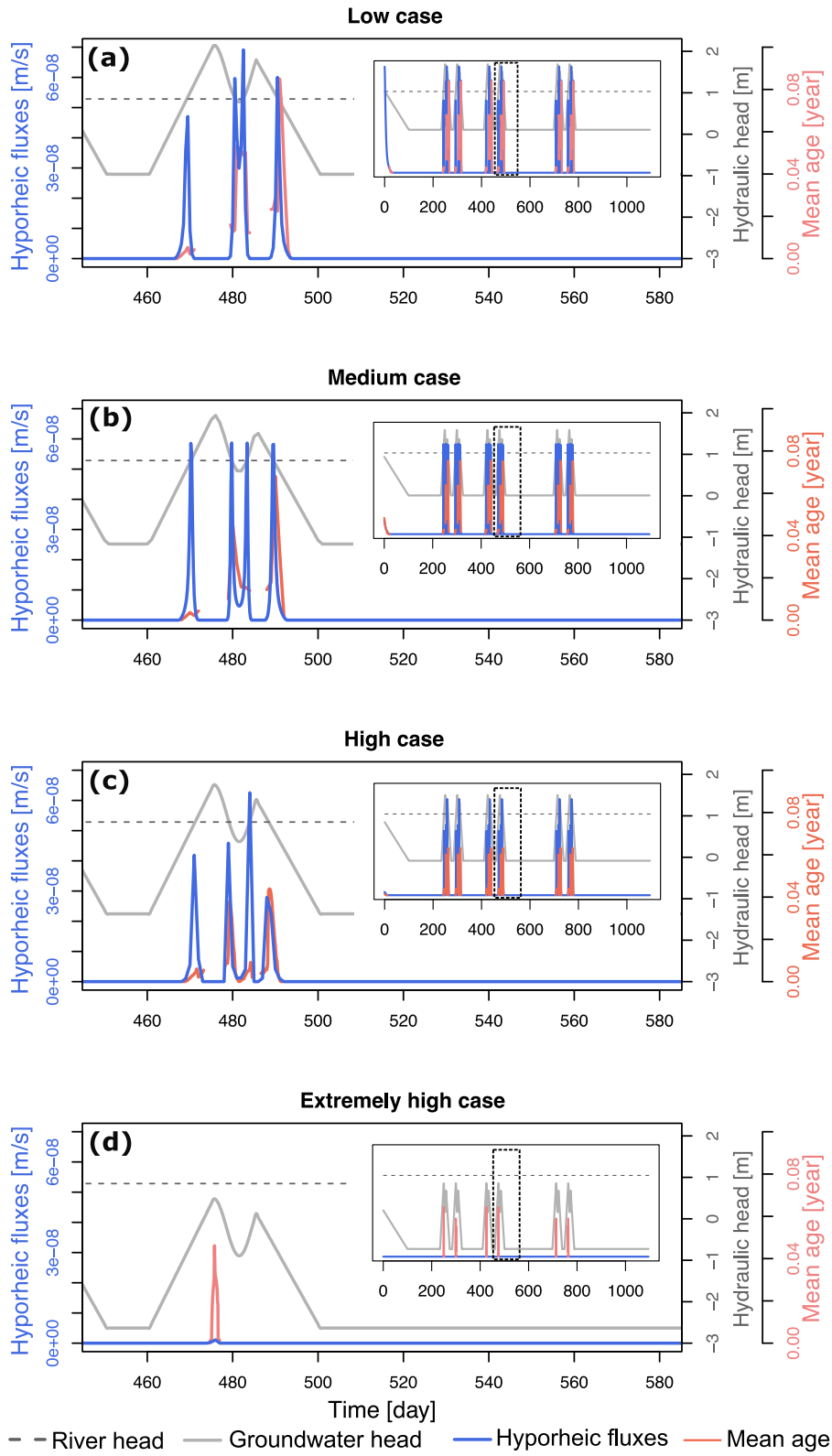

Figure 5. Hyporheic exchange fluxes and mean age at different levels of surface water groundwater disconnection for atmospheric river scenario.

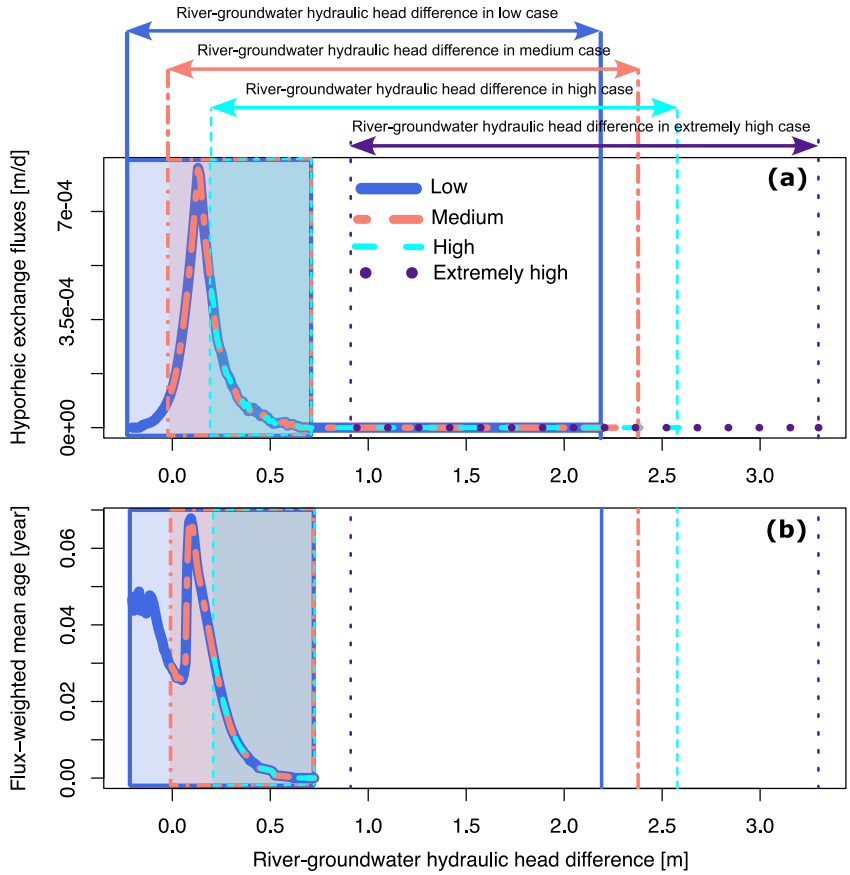

Figure 6. (a) Hyporheic exchange fluxes and (b) flux-weighted mean age as a function of river groundwater hydraulic head gradient (i.e., head at the water-sediment interface minus head at the bottom of the modeling domain) for the groundwater average scenario.

in addition to the increased frequency of peaks, is the increased sharpness of the peaks, which was associated with the increase in speed of the change in groundwater head conditions.

3.2.3. Intermittency and Sensitivity of Bedform-Induced Hyporheic Exchange Fluxes

Bedform-induced hyporheic exchange only occurs intermittently when there are small or negligible differences between river and groundwater heads and can be non-existent when there are increased differences between river and groundwater heads. The extremely high case, in particular, results in a condition where the bedform-induced hyporheic zone cannot form because the head gradient between the channel and the aquifer results in losing fluxes to the regional aquifer that continually suppress the formation of hyporheic circulation cells. This intermittency responds to the seasonal- and event-scale groundwater hydraulic head variations. Only when the gaining and losing fluxes are low or negligible can bedform-induced hyporheic fluxes occur.

Our results also suggest that hyporheic flux has vast changes in magnitude, indicating the sensitivity of hyporheic exchange responding to the seasonal- and event-scale hydraulic head variations. The temporal frequency of the intersections between surface water and groundwater hydraulic heads controls the number and frequency of the hyporheic zone formations. The slope of the rising and falling limbs of groundwater table fluctuations determines the magnitude of hyporheic exchange fluxes and the flux-weighted mean age (Figures 4 and 5).

3.3. Windows for Hyporheic Exchange Occurrence

To further analyze under which range of river-groundwater head differences hyporheic exchange occurs, we plot the hyporheic exchange fluxes (Figure 6a) and flux-weighted mean ages (Figure 6b) as a function of river-groundwater head differences for the groundwater average scenario. Given the periodic and non-hysteretic

nature of this process, we explored a single year, starting when the groundwater table is at its deepest (i.e., the largest positive value of the hydraulic head difference). The full range of head difference considered for each case is indicated by the vertical lines on the plots, and the windows where the hyporheic zone is active are illustrated by the shaded areas.

Initially, the positive gradient induces losing conditions, with regional groundwater fluxes strong enough to completely suppress bedform-induced hyporheic exchange. Over time, as the gradient progressively decreases (i.e., the groundwater head at the bottom boundary increases), it reaches a threshold where the hyporheic zone can overcome the compressing effect of the downward regional groundwater flow to form a hyporheic cell. This is the beginning of the rising limb for the exchange flux and mean age (moving from left to right in Figures 6a and 6b).

The exchange flux and mean age eventually reach a maximum, which depends on the water table dynamics for each case. For example, the low and medium cases reach the maximum exchange flux and mean age before the gradient momentarily reverses (see Figure 2). This "sweet spot" occurs at a head difference of approximately 0.13 m and not when the head difference is zero, which is likely explained by the delayed propagation of the hydraulic signal in a partially saturated porous media. Smaller head differences are characterized by lower exchange fluxes and mean ages, even after the head reversal. Notice that for the low case, the head reversal is strong enough to temporarily compress the hyporheic zone. However, the mean ages remain high and even increase due to the mixing of older groundwater and fresh surface water under gaining conditions (Figure 6b). Then, the cycle continues with a receding water table, and the fluxes follow the same path until the bedform-induced hyporheic zone disappears again.

Our results show that a peak exchange flux and mean age occurs near the zero difference in the hydraulic head, and the exchange becomes negligible when the head difference exceeds approximately 0.6 m (for the hydraulic properties used herein). Only when the head difference is below this threshold (inside the shaded areas) the hyporheic zone is active. This narrow range of hyporheic zone activity can be understood as a hot moment for biogeochemical activity (McClain et al., 2003) and highlights the fragility of the bedform-induced hyporheic zone, as it only exists when the head differences between the river and groundwater are small. When the hydraulic gradient is too large under losing conditions, the river water that infiltrates into the streambed sediments is lost permanently and not able to return to the river. Under gaining conditions, when the hydraulic gradient is too large, the stream water is unable to infiltrate into the streambed sediments.

These findings are consistent with the descriptions in prior papers. For example, O'Connor and Harvey (2008) showed that groundwater upwelling in field measurements deviates from advective pumping and diffusive mass transfer scaling developed from lab flume studies, which suggests the fragility of hyporheic exchange when modulated by changing hydraulic gradients. Similarly, in a recent study, Bonanno et al. (2023) showed that the dynamics of regional groundwater fluxes can lead to periods where the exchange process is undetectable in tracer tests. Most rivers and streams are gaining or losing (Wroblicky et al., 1998) and are likely to inhibit the formation of bedform-induced hyporheic exchange. In fact, this inhibition is likely to become more prevalent in the future due to the widespread presence of losing conditions in river channels across the contiguous USA (Jasechko et al., 2021), with many basins expected to have increased future water shortages associated with the combined effects of population growth and climate change in the U.S. (Heidari et al., 2021), a factor that could further decrease river flows and increase intermittency in the U.S. and around the globe.

3.4. The Fragility of the Hyporheic Zone

Bedform-induced advective pumping is at the core of most upscaling frameworks for hyporheic exchange. While not the only exchange driver, it has become the common conceptualization for the hyporheic exchange processes. However, as shown here, this process can easily succumb to ubiquitous regional groundwater fluxes, likely limiting its overall role in river corridor biogeochemical transformations.

Note that the river sediment scenario and the groundwater table fluctuation patterns are generalized based on arid and semi-arid environments. However, the conclusions are transferable in other types of environments. Without a perched stream, the sensitivity of the bedform-induced hyporheic zone is still very high to the groundwater table fluctuations as noted in previous studies (Boano et al., 2008; Cardenas & Wilson, 2006; Sawyer & Cardenas, 2012). In wetter environments, the hyporheic exchange can also be deactivated as soon as the river-aquifer

hydraulic gradients are larger than a threshold. As discussed in the previous results, bedform-induced hyporheic exchange is obliterated by minor losing conditions well in advance of the disconnection between rivers and groundwater. Therefore, the hyporheic zones are likely to be fragile as well in other types of environments as in the arid and semi-arid regions.

The fragility of bedform-induced advective pumping emphasizes the importance and need for more research attention and considerations of other types of hyporheic exchanges, that is, near-bed turbulence and turnover (Grant et al., 2018; Nagaoka & Ohgaki, 1990; Roche et al., 2018; Schulz et al., 2023). Although these two types of hyporheic exchange may also potentially be affected by large gradients between surface water and groundwater hydraulic heads, there is still a lack of evidence to quantify how fragile these processes would be. For example, mass exchange rates in flat gravel beds have been found to be 2–4 orders of magnitude greater than those predicted by advective pumping, which is negligible in streambeds with small topographic features (O'Connor & Harvey, 2008; Packman et al., 2004; Roche et al., 2018) or under the modulating effect of regional groundwater flow, as shown in this study. The turbulent exchange of mass and momentum is likely more persistent and independent of groundwater table fluctuations and can potentially play an important role in sustaining the biogeochemical and ecological functioning of the river-aquifer system. Apart from the vertical hyporheic exchange processes, river channel meander-driven hyporheic exchange also plays an important role. A recent study reported that meander-driven hyporheic exchanges exhibit relatively more resilience to the regional groundwater table fluctuations (Gonzalez-Duque et al., 2024).

4. Conclusions

In this paper, we evaluate the persistence of bedform-induced advective pumping hyporheic exchange (bedform-induced exchange) under a range of seasonal- and event-scale groundwater table fluctuation scenarios, which lead to episodic river-aquifer disconnections and reconnections. Our study shows that this exchange mechanism, commonly assumed as ubiquitous, is highly sensitive to typical changes in groundwater table fluctuations and stream-aquifer disconnections. Such water table dynamics are particularly common in arid and semi-arid environments, but the presence of strong losing and disconnected channels is common in humid environments and is expected to expand due to climatic and anthropogenic drivers (e.g., Jasechko et al., 2021).

Bedform-induced exchange only occurs under conditions when the river head is not significantly different from the groundwater head, resulting in a fragile exchange mechanism that is either intermittent or absent under typical groundwater dynamics. When a bedform-induced hyporheic zone forms, typically during a short window of time, it is characterized by fluxes and mean water ages with significant peaks that vary by orders of magnitude. This intermittent process can be associated with the emergence of hot spots and hot moments of enhanced hyporheic zone biogeochemical reactivity along river corridors.

We propose that the fragility of bedform-induced hyporheic exchange highlights the importance of expanding typical conceptualizations to better represent the potential role of near-bed turbulence and turnover mechanisms when representing hyporheic connectivity in water quality models (e.g., Grant et al., 2018, 2020).

Acknowledgments
This research was funded by the U.S. Department of Energy, Office of Science, Biological and Environmental Research. This work is a product of three programs: (a) Environmental System Science Program, as part of the Watershed Dynamics and Evolution (WaDE) Science Focus Area at Oak Ridge National Laboratory, and the IDEAS-Watersheds project, (b) Data Management Program, as part of the ExaSheds project, (c) the Research and Development Partnership Pilots (DE-SC0023132), and (d) ORNL SEED project: Tracking Disturbance Signals Along River Networks. Additional support was provided by the Department of Energy Minority Serving Institution Partnership Program (MSIPP) managed by the Savannah River National Laboratory and National Science Foundation (awards 2142686, 1830172, 2020814, 2312326).

Data Availability Statement

The data and R scripts needed to reproduce the analyses and figures in this study are available through FigShare: https://figshare.com/s/3c8a2d5ce9e8185602f7.

References

Azizian, M., Boano, F., Cook, P. L., Detwiler, R. L., Rippy, M. A., & Grant, S. B. (2017). Ambient groundwater flow diminishes nitrate processing in the hyporheic zone of streams. *Water Resources Research*, *53*(5), 3941–3967. https://doi.org/10.1002/2016wr020048

Azizian, M., Grant, S. B., Kessler, A. J., Cook, P. L. M., Rippy, M. A., & Stewardson, M. J. (2015). Bedforms as biocatalytic filters: A pumping and streamline segregation model for nitrate removal in permeable sediments. *Environmental Science & Technology*, *49*(18), 10993–11002. https://doi.org/10.1021/acs.est.5b01941

Bear, J. (1972). *Dynamics of fluids in porous media*. American Elsevier Publishing.

Boano, F., De Falco, N., & Arnon, S. (2018). Modeling chemical gradients in sediments under losing and gaining flow conditions: The GRADIENT code. *Advances in Water Resources*, *112*, 72–82. https://doi.org/10.1016/j.advwatres.2017.12.002

Boano, F., Harvey, J. W., Marion, A., Packman, A. I., Revelli, R., Ridolfi, L., & Wörman, A. (2014). Hyporheic flow and transport processes: Mechanisms, models, and biogeochemical implications. *Reviews of Geophysics*, *52*(4), 603–679. https://doi.org/10.1002/2012rg000417

Boano, F., Revelli, R., & Ridolfi, L. (2008). Reduction of the hyporheic zone volume due to the stream-aquifer interaction. *Geophysical Research Letters*, *35*(9), L09401. https://doi.org/10.1029/2008gl033554

Boano, F., Revelli, R., & Ridolfi, L. (2009). Quantifying the impact of groundwater discharge on the surface-subsurface exchange. *Hydrological Processes*, *23*(15), 2108–2116. https://doi.org/10.1002/hyp.7278
Bonanno, E., Blöschl, G., & Klaus, J. (2023). Discharge, groundwater gradients, and streambed micro-topography control the temporal dynamics of transient storage in a headwater reach. *Water Resources Research*, *59*(7), e2022WR034053. https://doi.org/10.1029/2022WR034053
Boulton, A. J. (2003). Parallels and contrasts in the effects of drought on stream macroinvertebrate assemblages. *Freshwater Biology*, *48*(7), 1173–1185. https://doi.org/10.1046/j.1365-2427.2003.01084.x
Bridge, J. S. (2003). *Rivers and floodplains: Forms, processes, and sedimentary record*. John Wiley & Sons.
Briggs, M. A., Lautz, L. K., & Hare, D. K. (2014). Residence time control on hot moments of net nitrate production and uptake in the hyporheic zone. *Hydrological Processes*, *28*(11), 3741–3751. https://doi.org/10.1002/hyp.9921
Brunner, P., Cook, P. G., & Simmons, C. T. (2009). Hydrogeologic controls on disconnection between surface water and groundwater. *Water Resources Research*, *45*(1). https://doi.org/10.1029/2008wr006953
Brunner, P., Cook, P. G., & Simmons, C. T. (2011). Disconnected surface water and groundwater: From theory to practice. *Ground Water*, *49*(4), 460–467. https://doi.org/10.1111/j.1745-6584.2010.00752.x
Brunner, P., Simmons, C. T., & Cook, P. G. (2009). Spatial and temporal aspects of the transition from connection to disconnection between rivers, lakes and groundwater. *Journal of Hydrology*, *376*(1–2), 159–169. https://doi.org/10.1016/j.jhydrol.2009.07.023
Buffington, J. M., & Tonina, D. (2009). Hyporheic exchange in mountain rivers II: Effects of channel morphology on mechanics, scales, and rates of exchange. *Geography Compass*, *3*(3), 1038–1062. https://doi.org/10.1111/j.1749-8198.2009.00225.x
BV, C., & OY, C. (1998). *Comsol multiphysics user's guide © copyright 1998–2010*. Comsol ab.
Cardenas, M. B. (2007). Potential contribution of topography-driven regional groundwater flow to fractal stream chemistry: Residence time distribution analysis of Tóth flow. *Geophysical Research Letters*, *34*(5), 5. https://doi.org/10.1029/2006GL029126
Cardenas, M. B. (2008). Surface water-groundwater interface geomorphology leads to scaling of residence times. *Geophysical Research Letters*, *35*(8), L08402. https://doi.org/10.1029/2008GL033753
Cardenas, M. B., & Wilson, J. (2006). The influence of ambient groundwater discharge on exchange zones induced by current–bedform interactions. *Journal of Hydrology*, *331*(1–2), 103–109. https://doi.org/10.1016/j.jhydrol.2006.05.012
Cardenas, M. B., & Wilson, J. (2007a). Exchange across a sediment–water interface with ambient groundwater discharge. *Journal of Hydrology*, *346*(3–4), 69–80. https://doi.org/10.1016/j.jhydrol.2007.08.019
Cardenas, M. B., & Wilson, J. (2007b). Hydrodynamics of coupled flow above and below a sediment–water interface with triangular bedforms. *Advances in Water Resources*, *30*(3), 301–313. https://doi.org/10.1016/j.advwatres.2006.06.009
Caruso, A., Ridolfi, L., & Boano, F. (2016). Impact of watershed topography on hyporheic exchange. *Advances in Water Resources*, *94*, 400–411. https://doi.org/10.1016/j.advwatres.2016.06.005
Claret, C., & Boulton, A. J. (2009). Integrating hydraulic conductivity with biogeochemical gradients and microbial activity along river-groundwater exchange zones in a subtropical stream. *Hydrogeology Journal*, *17*(1), 151–160. https://doi.org/10.1007/s10040-008-0373-3
Elliott, A. H., & Brooks, N. H. (1997). Transfer of nonsorbing solutes to a streambed with bed forms: Laboratory experiments. *Water Resources Research*, *33*(1), 137–151. https://doi.org/10.1029/96wr02783
Findlay, S. (1995). Importance of surface-subsurface exchange in stream ecosystems: The hyporheic zone. *Limnology & Oceanography*, *40*(1), 159–164. https://doi.org/10.4319/lo.1995.40.1.0159
Fuchs, E. H., King, J. P., & Carroll, K. C. (2019). Quantifying disconnection of groundwater from managed-ephemeral surface water during drought and conjunctive agricultural use. *Water Resources Research*, *55*(7), 5871–5890. https://doi.org/10.1029/2019wr024941
Ginn, T. (1999). On the distribution of multicomponent mixtures over generalized exposure time in subsurface flow and reactive transport: Foundations, and formulations for groundwater age, chemical heterogeneity, and biodegradation. *Water Resources Research*, *35*(5), 1395–1407. https://doi.org/10.1029/1999wr900013
Gómez-Gener, L., Siebers, A. R., Arce, M. I., Arnon, S., Bernal, S., Bolpagni, R., et al. (2021). Towards an improved understanding of biogeochemical processes across surface-groundwater interactions in intermittent rivers and ephemeral streams. *Earth-Science Reviews*, *220*, 103724. https://doi.org/10.1016/j.earscirev.2021.103724
Gomez-Velez, J. D., & Harvey, J. W. (2014a). A hydrogeomorphic river network model predicts where and why hyporheic exchange is important in large basins. *Geophysical Research Letters*, *41*(18), 2014GL061099. https://doi.org/10.1002/2014GL061099
Gomez-Velez, J. D., & Harvey, J. W. (2014b). A hydrogeomorphic river network model predicts where and why hyporheic exchange is important in large basins. *Geophysical Research Letters*, *41*(18), 6403–6412. https://doi.org/10.1002/2014gl061099
Gomez-Velez, J. D., Harvey, J. W., Cardenas, M. B., & Kiel, B. (2015). Denitrification in the Mississippi River network controlled by flow through river bedforms. *Nature Geoscience*, *8*(12), 941–945. https://doi.org/10.1038/ngeo2567
Gomez-Velez, J. D., Krause, S., & Wilson, J. L. (2014). Effect of low-permeability layers on spatial patterns of hyporheic exchange and groundwater upwelling. *Water Resources Research*, *50*(6), 5196–5215. https://doi.org/10.1002/2013WR015054
Gomez-Velez, J. D., & Wilson, J. L. (2013). Age distributions and dynamically changing hydrologic systems: Exploring topography-driven flow. *Water Resources Research*, *49*(3), 1503–1522. https://doi.org/10.1002/wrcr.20127
Gomez-Velez, J. D., Wilson, J. L., Cardenas, M. B., & Harvey, J. W. (2017). Flow and residence times of dynamic river bank storage and sinuosity-driven hyporheic exchange. *Water Resources Research*, *53*(10), 8572–8595. https://doi.org/10.1002/2017WR021362
Gonzalez-Duque, D., Gomez-Velez, J. D., Zarnetske, J. P., Chen, X., & Scheibe, T. D. (2024). Sinuosity-driven hyporheic exchange: Hydrodynamics and biogeochemical potentials. *Water Resources Research*, *60*(4), e2023WR036023. https://doi.org/10.1029/2023wr036023
Gooseff, M. N. (2010). Defining hyporheic zones–advancing our conceptual and operational definitions of where stream water and groundwater meet. *Geography Compass*, *4*(8), 945–955. https://doi.org/10.1111/j.1749-8198.2010.00364.x
Grant, S. B., Gomez-Velez, J. D., & Ghisalberti, M. (2018). Modeling the effects of turbulence on hyporheic exchange and local-to-global nutrient processing in streams. *Water Resources Research*, *54*(9), 5883–5889. https://doi.org/10.1029/2018wr023078
Grant, S. B., Monofy, A., Boano, F., Gomez-Velez, J. D., Guymer, I., Harvey, J., & Ghisalberti, M. (2020). Unifying advective and diffusive descriptions of bedform pumping in the benthic biolayer of streams. *Water Resources Research*, *56*(11), e2020WR027967. https://doi.org/10.1029/2020wr027967
Gu, C., Anderson, W., & Maggi, F. (2012). Riparian biogeochemical hot moments induced by stream fluctuations. *Water Resources Research*, *48*(9). https://doi.org/10.1029/2011wr011720
Hammond, J. C., Zimmer, M., Shanafield, M., Kaiser, K., Godsey, S. E., Mims, M. C., et al. (2021). Spatial patterns and drivers of nonperennial flow regimes in the contiguous United States. *Geophysical Research Letters*, *48*(2), e2020GL090794. https://doi.org/10.1029/2020gl090794
Harvey, J., Gomez-Velez, J., Schmadel, N., Scott, D., Boyer, E., Alexander, R., et al. (2018). How hydrologic connectivity regulates water quality in river corridors. *JAWRA Journal of the American Water Resources Association*, *55*(2), 369–381. https://doi.org/10.1111/1752-1688.12691

Harvey, J., & Gooseff, M. (2015). River corridor science: Hydrologic exchange and ecological consequences from bedforms to basins. *Water Resources Research*, *51*(9), 6893–6922. https://doi.org/10.1002/2015wr017617

Heidari, H., Arabi, M., & Warziniack, T. (2021). Vulnerability to water shortage under current and future water supply-demand conditions across U.S. River basins. *Earth's Future*, *9*(10), e2021EF002278. https://doi.org/10.1029/2021EF002278

Herzog, S. P., Ward, A. S., & Wondzell, S. M. (2019). Multiscale feature-feature interactions control patterns of hyporheic exchange in a simulated headwater mountain stream. *Water Resources Research*, *55*(12), 10976–10992. https://doi.org/10.1029/2019WR025763

Hester, E. T., Cardenas, M. B., Haggerty, R., & Apte, S. V. (2017). The importance and challenge of hyporheic mixing. *Water Resources Research*, *53*(5), 3565–3575. https://doi.org/10.1002/2016wr020005

Hester, E. T., Young, K., & Widdowson, M. A. (2013). Mixing of surface and groundwater induced by riverbed dunes: Implications for hyporheic zone definitions and pollutant reactions. *Water Resources Research*, *49*(9), 5221–5237. https://doi.org/10.1002/wrcr.20399

Irvine, D. J., Brunner, P., Franssen, H.-J. H., & Simmons, C. T. (2012). Heterogeneous or homogeneous? Implications of simplifying heterogeneous streambeds in models of losing streams. *Journal of Hydrology*, *424*, 16–23. https://doi.org/10.1016/j.jhydrol.2011.11.051

Jasechko, S., Seybold, H., Perrone, D., Fan, Y., & Kirchner, J. W. (2021). Widespread potential loss of streamflow into underlying aquifers across the USA. *Nature*, *591*(7850), 391–395. https://doi.org/10.1038/s41586-021-03311-x

Krause, S., Abbott, B. W., Baranov, V., Bernal, S., Blaen, P., Datry, T., et al. (2022). Organizational principles of hyporheic exchange flow and biogeochemical cycling in river networks across scales. *Water Resources Research*, *58*(3), e2021WR029771. https://doi.org/10.1029/2021wr029771

Krause, S., Hannah, D. M., Fleckenstein, J., Heppell, C., Kaeser, D., Pickup, R., et al. (2011). Inter-disciplinary perspectives on processes in the hyporheic zone. *Ecohydrology*, *4*(4), 481–499. https://doi.org/10.1002/eco.176

Krause, S., Lewandowski, J., Grimm, N. B., Hannah, D. M., Pinay, G., McDonald, K., et al. (2017). Ecohydrological interfaces as hot spots of ecosystem processes. *Water Resources Research*, *53*(8), 6359–6376. https://doi.org/10.1002/2016WR019516

Malzone, J. M., Anseeuw, S. K., Lowry, C. S., & Allen-King, R. (2016). Temporal hyporheic zone response to water table fluctuations. *Ground Water*, *54*(2), 274–285. https://doi.org/10.1111/gwat.12352

Marzadri, A., Tonina, D., & Bellin, A. (2011). A semianalytical three-dimensional process-based model for hyporheic nitrogen dynamics in gravel bed rivers. *Water Resources Research*, *47*(11), W11518. https://doi.org/10.1029/2011WR010583

Marzadri, A., Tonina, D., McKean, J. A., Tiedemann, M. G., & Benjankar, R. M. (2014). Multi-scale streambed topographic and discharge effects on hyporheic exchange at the stream network scale in confined streams. *Journal of Hydrology*, *519*, 1997–2011. https://doi.org/10.1016/j.jhydrol.2014.09.076

McClain, M. E., Boyer, E. W., Dent, C. L., Gergel, S. E., Grimm, N. B., Groffman, P. M., et al. (2003). Biogeochemical hot spots and hot moments at the interface of terrestrial and aquatic ecosystems. *Ecosystems*, *6*(4), 301–312. https://doi.org/10.1007/s10021-003-0161-9

Menter, F. R. (1994). Two-equation eddy-viscosity turbulence models for engineering applications. *AIAA Journal*, *32*(8), 1598–1605. https://doi.org/10.2514/3.12149

Millington, R. J., & Quirk, J. P. (1961). Permeability of porous solids. *Transactions of the Faraday Society*, *57*(0), 1200–1207. https://doi.org/10.1039/TF9615701200

Nagaoka, H., & Ohgaki, S. (1990). Mass transfer mechanism in a porous riverbed. *Water Research*, *24*(4), 417–425. https://doi.org/10.1016/0043-1354(90)90223-s

Newcomer, M. E., Hubbard, S. S., Fleckenstein, J. H., Maier, U., Schmidt, C., Thullner, M., et al. (2018). Influence of hydrological perturbations and riverbed sediment characteristics on hyporheic zone respiration of CO_2 and N_2. *Journal of Geophysical Research: Biogeosciences*, *123*(3), 902–922. https://doi.org/10.1002/2017jg004090

O'Connor, B. L., & Harvey, J. W. (2008). Scaling hyporheic exchange and its influence on biogeochemical reactions in aquatic ecosystems. *Water Resources Research*, *44*(12). https://doi.org/10.1029/2008wr007160

Packman, A. I., Salehin, M., & Zaramella, M. (2004). Hyporheic exchange with gravel beds: Basic hydrodynamic interactions and bedform-induced advective flows. *Journal of Hydraulic Engineering*, *130*(7), 647–656. https://doi.org/10.1061/(asce)0733-9429(2004)130:7(647)

Pearson, A. J., Rucker, D. F., Tsai, C.-H., Fuchs, E. H., & Carroll, K. C. (2022). Electrical resistivity monitoring of lower Rio Grande river-groundwater intermittency. *Journal of Hydrology*, *613*, 128325. https://doi.org/10.1016/j.jhydrol.2022.128325

Perez, G., Gomez-Velez, J. D., Chen, X., Scheibe, T., Chen, Y., & Bao, J. (2021). Identification of characteristic spatial scales to improve the performance of analytical spectral solutions to the groundwater flow equation. *Water Resources Research*, *57*(12), e2021WR031044. https://doi.org/10.1029/2021WR031044

Quichimbo, E. A., Singer, M. B., & Cuthbert, M. O. (2020). Characterising groundwater–surface water interactions in idealised ephemeral stream systems. *Hydrological Processes*, *34*(18), 3792–3806. https://doi.org/10.1002/hyp.13847

Richards, L. A. (1931). Capillary conduction of liquids through porous mediums. *Physics*, *1*(5), 318–333. https://doi.org/10.1063/1.1745010

Rivière, A., Gonçalvès, J., Jost, A., & Font, M. (2014). Experimental and numerical assessment of transient stream–aquifer exchange during disconnection. *Journal of Hydrology*, *517*, 574–583. https://doi.org/10.1016/j.jhydrol.2014.05.040

Roche, K., Blois, G., Best, J., Christensen, K., Aubeneau, A., & Packman, A. (2018). Turbulence links momentum and solute exchange in coarse-grained streambeds. *Water Resources Research*, *54*(5), 3225–3242. https://doi.org/10.1029/2017wr021992

Sawyer, A. H., & Cardenas, M. B. (2012). Effect of experimental wood addition on hyporheic exchange and thermal dynamics in a losing meadow stream. *Water Resources Research*, *48*(10). https://doi.org/10.1029/2011wr011776

Schulz, H., Teitelbaum, Y., Lewandowski, J., Singer, G. A., & Arnon, S. (2023). Moving bedforms control CO_2 production and distribution in Sandy River sediments. *Journal of Geophysical Research: Biogeosciences*, *128*(4), e2022JG007156. https://doi.org/10.1029/2022JG007156

Shabaga, J. A., & Hill, A. R. (2010). Groundwater-fed surface flow path hydrodynamics and nitrate removal in three riparian zones in southern Ontario, Canada. *Journal of Hydrology*, *388*(1–2), 52–64. https://doi.org/10.1016/j.jhydrol.2010.04.028

Shanafield, M., Cook, P. G., Brunner, P., McCallum, J., & Simmons, C. T. (2012). Aquifer response to surface water transience in disconnected streams. *Water Resources Research*, *48*(11). https://doi.org/10.1029/2012wr012103

Son, K., Fang, Y., Gomez-Velez, J. D., Byun, K., & Chen, X. (2022). Combined effects of stream hydrology and land use on basin-scale hyporheic zone denitrification in the Columbia River basin. *Water Resources Research*, *58*(12), e2021WR031131. https://doi.org/10.1029/2021WR031131

Son, K., Fang, Y., Gomez-Velez, J. D., & Chen, X. (2022). Spatial microbial respiration variations in the hyporheic zones within the Columbia River basin. *Journal of Geophysical Research: Biogeosciences*, *127*(11), e2021JG006654. https://doi.org/10.1029/2021JG006654

Stanley, E. H., Fisher, S. G., & Grimm, N. B. (1997). Ecosystem expansion and contraction in streams. *BioScience*, *47*(7), 427–435. https://doi.org/10.2307/1313058

Stegen, J. C., Fredrickson, J. K., Wilkins, M. J., Konopka, A. E., Nelson, W. C., Arntzen, E. V., et al. (2016). Groundwater–surface water mixing shifts ecological assembly processes and stimulates organic carbon turnover. *Nature Communications*, *7*(1), 11237. https://doi.org/10.1038/ncomms11237

Stegen, J. C., Johnson, T., Fredrickson, J. K., Wilkins, M. J., Konopka, A. E., Nelson, W. C., et al. (2018). Influences of organic carbon speciation on hyporheic corridor biogeochemistry and microbial ecology. *Nature Communications*, *9*(1), 585. https://doi.org/10.1038/s41467-018-02922-9

Stephens, D. B. (1994). A perspective on diffuse natural recharge mechanisms in areas of low precipitation. *Soil Science Society of America Journal*, *58*(1), 40–48. https://doi.org/10.2136/sssaj1994.03615995005800010006x

Stonedahl, S. H., Harvey, J. W., Detty, J., Aubeneau, A., & Packman, A. I. (2012). Physical controls and predictability of stream hyporheic flow evaluated with a multiscale model. *Water Resources Research*, *48*(10). https://doi.org/10.1029/2011WR011582

Stonedahl, S. H., Harvey, J. W., & Packman, A. I. (2013). Interactions between hyporheic flow produced by stream meanders, bars, and dunes. *Water Resources Research*, *49*(9), 5450–5461. https://doi.org/10.1002/wrcr.20400

Stonedahl, S. H., Harvey, J. W., Wörman, A., Salehin, M., & Packman, A. I. (2010). A multiscale model for integrating hyporheic exchange from ripples to meanders. *Water Resources Research*, *46*(12). https://doi.org/10.1029/2009WR008865

Tonina, D., & Buffington, J. M. (2009). Hyporheic exchange in Mountain Rivers I: Mechanics and environmental effects. *Geography Compass*, *3*(3), 1063–1086. https://doi.org/10.1111/j.1749-8198.2009.00226.x

Tonina, D., & Buffington, J. M. (2011). Effects of stream discharge, alluvial depth and bar amplitude on hyporheic flow in pool-riffle channels. *Water Resources Research*, *47*(8). https://doi.org/10.1029/2010wr009140

Van Genuchten, M. T. (1980). A closed-form equation for predicting the hydraulic conductivity of unsaturated soils. *Soil Science Society of America Journal*, *44*(5), 892–898. https://doi.org/10.2136/sssaj1980.03615995004400050002x

Venditti, J. (2013). 9.10 bedforms in sand-bedded rivers. *Treatise on Geomorphology*, *9*, 137–162. https://doi.org/10.1016/b978-0-12-374739-6.00235-9

Wondzell, S. M. (2011). The role of the hyporheic zone across stream networks. *Hydrological Processes*, *25*(22), 3525–3532. https://doi.org/10.1002/hyp.8119

Wörman, A., Packman, A. I., Marklund, L., Harvey, J. W., & Stone, S. H. (2006). Exact three-dimensional spectral solution to surface-groundwater interactions with arbitrary surface topography. *Geophysical Research Letters*, *33*(7). https://doi.org/10.1029/2006gl025747

Wörman, A., Packman, A. I., Marklund, L., Harvey, J. W., & Stone, S. H. (2007). Fractal topography and subsurface water flows from fluvial bedforms to the continental shield. *Geophysical Research Letters*, *34*(7), L07402. https://doi.org/10.1029/2007gl029426

Wroblicky, G. J., Campana, M. E., Valett, H. M., & Dahm, C. N. (1998). Seasonal variation in surface-subsurface water exchange and lateral hyporheic area of two stream-aquifer systems. *Water Resources Research*, *34*(3), 317–328. https://doi.org/10.1029/97wr03285

Wu, L., Gomez-Velez, J. D., Krause, S., Singh, T., Wörman, A., & Lewandowski, J. (2020). Impact of flow alteration and temperature variability on hyporheic exchange. *Water Resources Research*, *56*(3). https://doi.org/10.1029/2019wr026225

Wu, L., Gomez-Velez, J. D., Krause, S., Wörman, A., Singh, T., Nützmann, G., & Lewandowski, J. (2021). How daily groundwater table drawdown affects the diel rhythm of hyporheic exchange. *Hydrology and Earth System Sciences*, *25*(4), 1905–1921. https://doi.org/10.5194/hess-25-1905-2021

Xian, Y., Jin, M., Liu, Y., & Si, A. (2017). Impact of lateral flow on the transition from connected to disconnected stream–aquifer systems. *Journal of Hydrology*, *548*, 353–367. https://doi.org/10.1016/j.jhydrol.2017.03.011

Xian, Y., Jin, M., Zhan, H., & Liu, Y. (2019). Reactive transport of nutrients and bioclogging during dynamic disconnection process of stream and groundwater. *Water Resources Research*, *55*(5), 3882–3903. https://doi.org/10.1029/2019wr024826

Xie, Y., Cook, P. G., Brunner, P., Irvine, D. J., & Simmons, C. T. (2014). When can inverted water tables occur beneath streams? *Ground Water*, *52*(5), 769–774. https://doi.org/10.1111/gwat.12109

Yalin, M. S. (1972). Mechanics of sediment transport. (No Title).

Yalin, M. S., & Da Silva, A. F. (2001). Fluvial processes.

Zipper, S. C., Hammond, J. C., Shanafield, M., Zimmer, M., Datry, T., Jones, C. N., et al. (2021). Pervasive changes in stream intermittency across the United States. *Environmental Research Letters*, *16*(8), 084033. https://doi.org/10.1088/1748-9326/ac14ec